

EFP SIMULATIONS WITH JOHNSON-COOK MODELS

Hervé Couque¹ and Rémi Boulanger¹

¹*Nexter Munitions, 7 route de Guerry, 18023 Bourges, France*

Because numerical simulations with classical Johnson-Cook formulation of explosively formed projectiles induce non representative projectiles, a modified Johnson-Cook model taking into account the thermally activated and viscous regimes as well as the notion of saturation stress in the 10^4 s^{-1} regime has been developed. Using both models, numerical experimental comparisons of Taylor and explosively formed projectiles tests are presented for a nickel and a high strength nickel alloy.

INTRODUCTION

When dealing with strain rates greater than 10^3 s^{-1} , the classical Johnson-Cook formulation (JC) [1] does not take into account the increase of the yield stress usually described by the viscous behaviour of the dislocations. In the case of explosively formed projectiles (EFP), where strain rates are ranging from 10^4 to 10^5 s^{-1} , such models induce non representative projectiles. One way to reproduce the projectile shape is to increase the hardening constants or to decrease the softening constant of the model.

A modified Johnson-Cook model (JCM) has been proposed to take into account the thermally activated and viscous regimes, that can be integrated in commercial numerical codes [2]. The model, calibrated using high strain rate data generated in the 10^3 s^{-1} regime with a split Hopkinson pressure bars technique and in the 10^4 - 10^5 s^{-1} regime with a direct impact Hopkinson pressure bar technique, was evaluated through the simulations of symmetric Taylor tests with the hydrocode AUTODYN [3]. At low impact speeds, numerical simulation of the Taylor specimens was improved with the use of the JCM model as shown in Figure 1. In an another hand, Taylor simulations at high impact speeds were found to underestimate the plastic deformation.

To improve simulations at high strain rates, a modification of the JCM model is proposed with the introduction of a saturation stress in the 10^4 s^{-1} strain rate regime as discussed by Steinberg et al [4]. The influence of the JC et JCM validation regimes was examined by comparing experimental and numerical results of Taylor and EFP tests for a nickel and a high strength nickel alloy. The numerical simulations were conducted

with AUTODYN with specific user subroutines for each JCM models as to implement the material modelling algorithm.

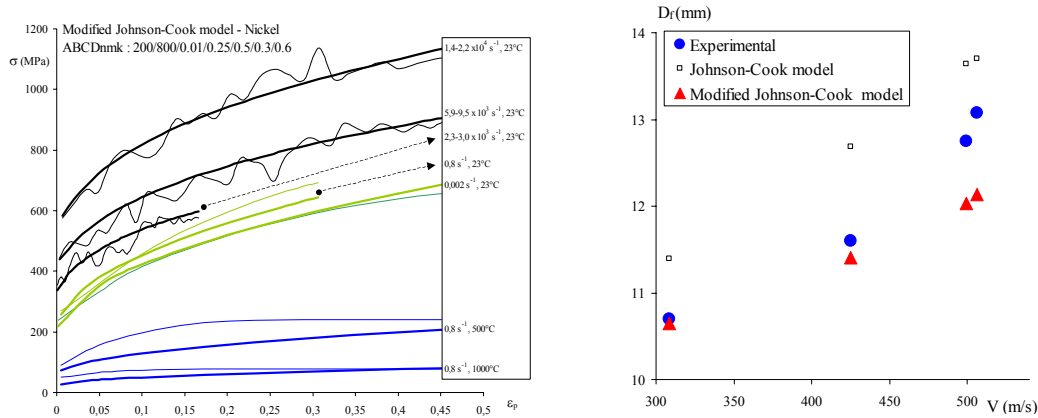


Figure 1. JCM model for a nickel: stress-strain response and final Taylor diameter [2].

MATERIALS AND MECHANICAL TESTS

The materials tested consist of a nickel, 200 MPa in yield stress, and a high strength nickel alloy, 345 MPa in yield stress and 10.6 g.cm^{-3} in density [2]. Conventional testing and split Hopkinson pressure bar techniques were used to generate data at strain rates ranging from 0.002 to 5000 s^{-1} and at temperatures ranging from 20 to 1000°C . A direct impact compression test was employed to obtain data in the viscous regime at strain rates varying from 10^3 to 10^4 s^{-1} . The technique consists in impacting at a constant velocity V a specimen placed against a Hopkinson pressure bar (HPB), see Figure 2. The true deformation $\epsilon(t)$ and the equivalent stress $\sigma(t)$ are given by :

$$\epsilon(t) = Ln(1 + \epsilon_n(t)) = Ln(1 + (Vt - C_o \int_0^t \epsilon_T(\tau) d\tau) / L_o) \tag{1}$$

$$\sigma(t) = \rho C_o^2 \epsilon_T(t) S_T/S_o (1 + \epsilon_n(t)) - (3/8) \rho (R_o V/L_o)^2 (1 - \epsilon_n(t))^3 \tag{2}$$

with L_o the specimen length, $\epsilon_T(t)$ the HPB strain history, C_o and ρ the sound velocity and density of the HPB material, S_T et S_o the HPB and specimen section [2].

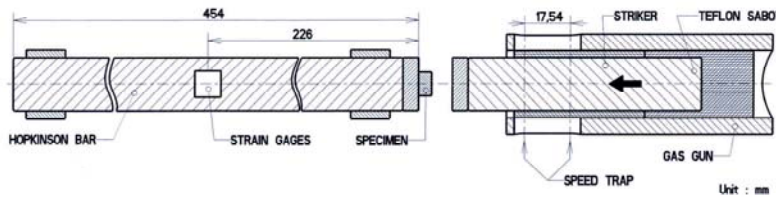


Figure 2. Direct impact compression test.

CONSTITUTIVE MODEL

The modified Johnson-Cook model includes a power strain rate component added to the logarithm strain rate term of the original Johnson-Cook formulation, $D(\dot{\epsilon} / \dot{\epsilon}_l)^k$, with D and k two constants. This component is normalized by a reference strain rate, $\dot{\epsilon}_l$, equal to 10^3 s^{-1} characterising the transition between the thermally activated regime and the viscous regime. The equivalent stress function of plastic strain, ϵ_p , strain rate, $\dot{\epsilon}$, and temperature, T , is expressed as :

$$\sigma = (A + B \epsilon_p^n) (1 + C \ln (\dot{\epsilon} / \dot{\epsilon}_0) + D(\dot{\epsilon} / \dot{\epsilon}_l)^k) (1 - [(T - T_r) / (T_m - T_r)]^m), \quad (3)$$

with the usual constants of the classical Johnson-Cook formulation: T_r , T_m the room and melting temperatures, $\dot{\epsilon}_0$, a reference strain rate equal to 1 s^{-1} and A , B , C , n , m five material constants describing the mechanical response. This formulation enables to go back to the classical when strain rates are lower than 10^3 s^{-1} , see Figure 3.

The model was compared to the Zerilli-Amstrong model (ZA) [5] for face-centered-cubic material. Both the ZA and JCM models reproduce the sharp turn of the strength observed in the 10^3 - 10^4 s^{-1} transition regime, see Figure 3. However, because the strain rate and temperature terms of the ZA model are coupled, the elevated temperature data cannot be reproduced. In the contrary, good agreement was reached both at high temperatures and high strain rates, for the JCM model, recall Figure 1 [2].

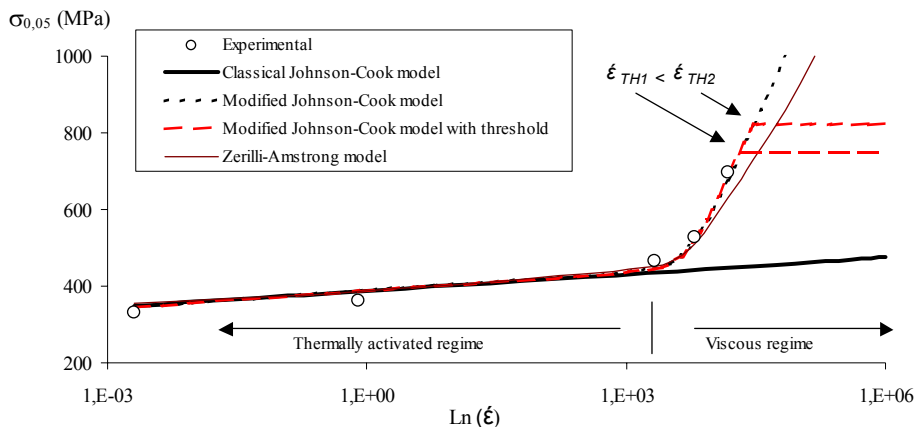


Figure 3. Constitutive model responses compared to experimental data for nickel at a plastic strain of 0.05.

Using Steinberg's argument which stipulates that at a given strain rate all effects of strain rate have saturated and the material strength becomes independent of strain rate, different threshold in strain rates, $\dot{\epsilon}_{TH}$, were investigated as shown in Figure 3.

VALIDATION TESTS

Two validation tests are considered. First, the direct impact compression test is revisited through comparisons of analytical and numerical responses. Second, the Taylor test is analyzed through experimental numerical comparisons. It is important to notice that Taylor tests of the nickel materials provide loading conditions approaching EFP, with an average plastic deformation of 0.4 and temperature of 500 K, and with strain rates ranging from 10^4 to 10^6 s⁻¹.

Simulation of direct impact compression tests

The stress strain response deduced from the analysis of the direct impact compression test, eqs. (1,2), was compared to numerical simulations for a nickel specimen impacted at 70.6 m.s⁻¹. The simulations were conducted with AUTODYN using a numerical model reproducing the complete set-up. An optimized specimen mesh size of 110 μ m was used [6].

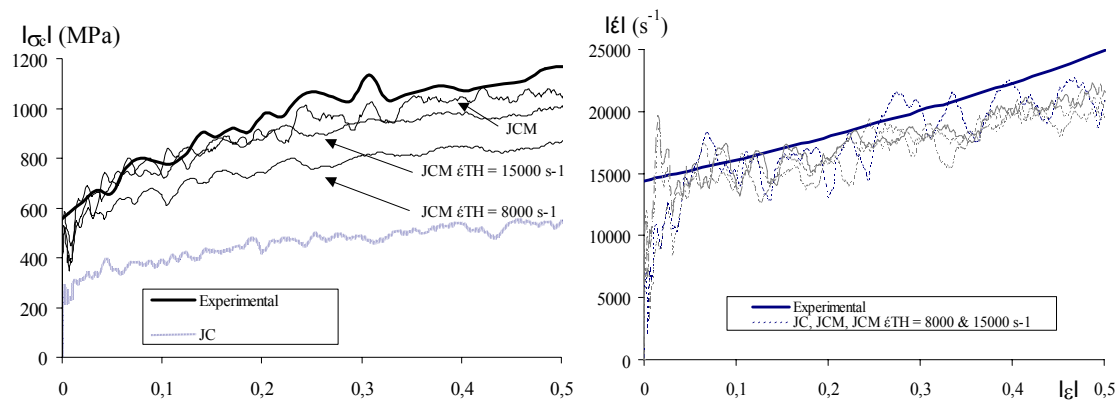


Figure 4. Stress-strain, strain rate-strain responses of a nickel specimen impacted at 70.6 m.s⁻¹.

As shown in Figure 4, the specimen stress deduced from the analytical formulation and numerical simulations with the JCM model is comparable. As expected with regard to the high strain rates reached in the compression test, right graph of Figure 4, the numerical simulation with JC model underestimates the stress. With the use of the JCM model with strain rate threshold, $\dot{\epsilon}_{TH}$, lower than in the experiment (8000, 15000 s⁻¹) the stress is again underestimated. As soon as a strain rate threshold of 20000 s⁻¹ is imposed, the JCM model (with and without strain rate threshold) gives the same response providing confidence in the use of JCM models.

Simulation of the symmetric Taylor tests

Numerical simulations of symmetric Taylor tests were conducted with AUTODYN for impact speeds ranging from 300 to 600 $\text{m}\cdot\text{s}^{-1}$. An optimized numerical model of the Taylor specimen was used composed of cells 100 μm in size in the plastically loaded region and 300 μm in size for the elastically loaded region [6].

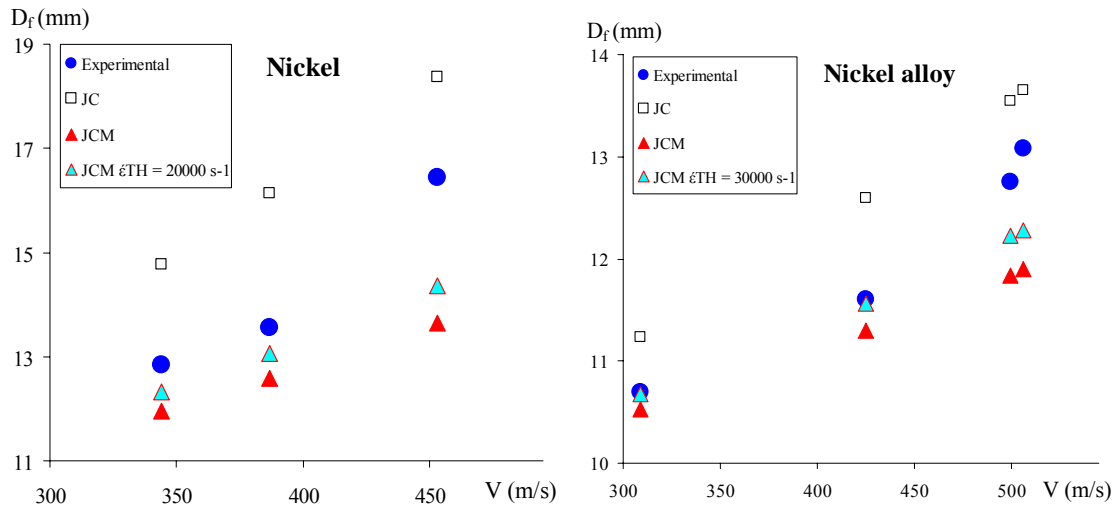


Figure 6. Final diameter of impact Taylor specimens versus impact speed.

Strength levelling observed at high impact speeds with the compression test has motivated the choice of strain rate thresholds of 20000 and 30000 s^{-1} for the nickel and nickel alloy, respectively. Simulations were conducted with three models: JC, JCM and JCM with the selected strain rate threshold. Figure 6 reports experimental and numerical final diameters of the Taylor specimens for both materials. The use of JC models with the strain rate threshold provides a better fit at high impact speeds. In fact for the nickel alloy, a perfect fit is obtained at low impact speeds. At high impact speeds, the diameter underestimate the diameter by only 6%. These results and the latest on the direct compression tests are encouraging and motivate EFP simulations.

EFP TESTS

A first approach to apply JCM models for very large strain and strain rate events is suggested with an EFP application. The aim is to compare numerical simulations with an experimental result for a nickel liner as to assess in which way the strain rate range modelled by the JCM model reproduce the EFP generation.

EFP testing configurations

An EFP charge 75 mm in caliber was used. The liner is placed against a HMX type explosive embedded in a steel cylinder closed by an aluminium plate, see Figure 7.

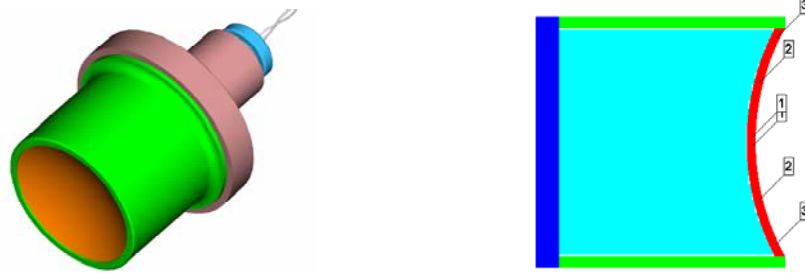


Figure 7. Schematic and numerical models of the EFP charge.

EFP numerical simulations

The numerical simulations of the EFP were performed with AUTODYN using a 2D-axisymmetrical model. An eulerian-lagrangian approach was used with an eulerian description of the explosive and a lagrangian description of the metallic parts. The steel body and the aluminium rear part of the EFP charge were modelled with elasto-plastic constitutive laws. The liner material was modelled with a Mie-Gruneisen equation of state coupled to the JC and JCM models. The explosive was modelled with a JWL equation coupled to the adapted detonation parameters of the explosive loading. A single point initiation in the centre of the charge was chosen for each simulation case.

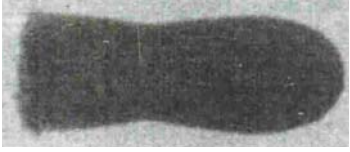
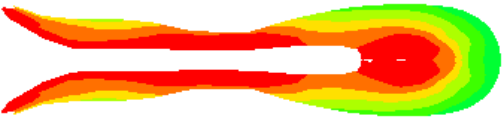
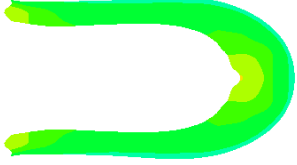
	<p><u>Experimental EFP</u></p> <p>Length = L_0 Diameter = D_0</p>
	<p><u>JC model</u></p> <p>$L/L_0 = 1.43$ $D/D_0 = 0.83$</p>
	<p><u>JCM model with $\dot{\epsilon}_{TH} = 20000 \text{ s}^{-1}$</u></p> <p>$L/L_0 = 0.80$ $D/D_0 = 1.17$</p>

Figure 8. Experimental and numerical EFP shapes.

Figure 8 reports the experimental and numerical results using a classical JC model and a JCM model with a strain rate threshold, $\dot{\epsilon}_{TH}$, of 20000 s^{-1} for the pure nickel. The consistency of these numerical results was investigated by doubling or dividing by two the meshing density in the thickness of the liner, corresponding to cell size ranging from 250 to 1000 μm . For both models, no significant variation of the numerical EFP sizes was observed.

Simulations with the JC model reveal an overestimation of the EFP length. As recalled by Figures 1 and 3, the sharp turn in strength observed in the 10^3 - 10^4 s^{-1} transition regime is not reproduced by the JC model. Such underestimation of the strength favours material softening resulting in elongated EFP and narrow EFP diameter. This is confirmed when strains are plotted as a function of strain rates, see Figure 9. Large strains exceeding 200% are recorded for the JC models associated with plastic instability at the extreme ends of the liner. It is important to notice that these plots confirmed the need for EFP to have material models reproducing the 10^4 - 10^5 s^{-1} strain rate regime.

An important difference on the shape of the simulated slug is obtained with the JCM model incorporating the strain rate threshold: material strengthening in the 10^3 - 10^4 s^{-1} strain rate regime gives a shorter EFP which is in length and diameter close to the experiment. This match goes along with a deformation rapidly becoming stable with plastic deformation less than 150%, see Figure 9.

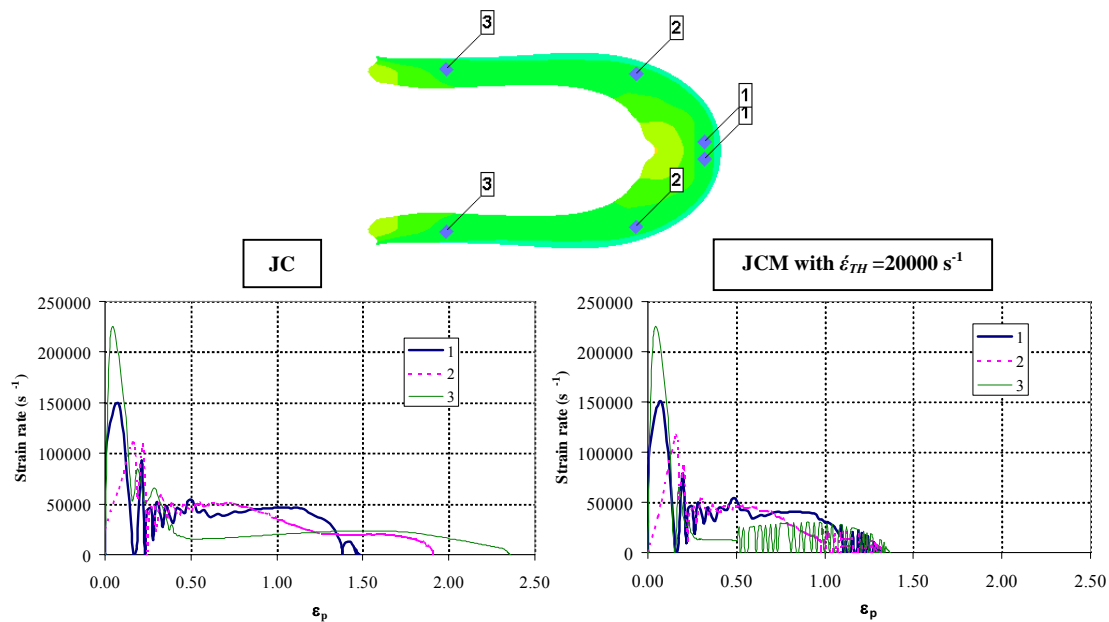


Figure 9. Strain rate-strain histories at three locations along the nickel liner using a JC model and a JCM model with strain rate threshold.

DISCUSSION

A modified Johnson-Cook constitutive model taking into account the strengthening observed in the thermally activated and viscous regimes as well as the notion of saturation stress in the 10^4 s^{-1} regime has been introduced. The model was validated at strain rates ranging from 10^4 to 10^6 s^{-1} using laboratory tests for deformation of 0.5 and temperature of 500 K.

The application of this model to large deformation under very high strain rates was investigated with the simulation of an explosively formed projectile. Currently, numerical simulations with classical Johnson-Cook model produce unrealistic elongated projectile shape, usually associated with plastic instability. With the use of modified Johnson-Cook model reproducing the strengthening at high strain rates, plastic deformation becomes quickly stable providing projectile with diameter and length comparable to the experiment.

The use of such models provides an excellent agreement when material are lightly shocked like in the Taylor test. However, the application to highly shocked materials as for explosively formed projectiles requires future investigations to take into account the influence of the shock intensity on yield and hardening characteristics. It is expected, that for nickel materials, the yield increase due to twinning formation during shock will lead to a decrease in hardening capacities at large strains. The incorporation of both effects in constitutive models will favor numerical modeling of the necking observed experimentally and provide improved simulations of the experimental diameter and length.

ACKNOWLEDGMENTS

The authors thank M Nicolas Eches for the implementation of the JCM models in AUTODYN.

REFERENCES

- [1] G. R. Johnson, W. H. Cook, A constitutive model and data for metals subjected to large strains, high strain rates and high temperatures, *7th International Symposium on Ballistics*, 541-548 (1983)
- [2] H. Couque, R. Boulanger, F. Bornet, A modified Johnson-Cook model for strain rates ranging from 10^{-3} to 10^{-5} s^{-1} , *DYMAT 2006 conference, Journal de Physique IV*, **134**, 87-93 (2006)
- [3] N. K. Bimbaum, M. S. Cowler, Numerical simulation of impact phenomena in an interactive computing environment, *IMPACT 1987 Conference, DGM*, 881-888 (1987)
- [4] D. J. Steinberg, S. G. Cochran S. G., M. W. Guinan, *J. Appl. Phys.*, **561**, 1498-1507 (1980)
- [5] R. W. Armstrong, F. J. Zerilli, Dislocation mechanics based analysis of material dynamics behavior, *DYMAT 1988 conference., Journal de Physique*, **49**, 529-534 (1988)
- [6] H. Couque, Symmetric Taylor testing procedures for material strength ranging from 400 to 2000 MPa, *DYMAT 2000 conference, Journal de Physique IV*, **10**, 179-184 (2000)